RESEARCH ARTICLE

An Inverted Sine Carrier PWM Strategy to Control the Photovoltaic Inverters Connected to Grid

Thoudeshetti Vishwagna[1], K. Mamatha[2]

[1]M.Tech Student (PE&D), Vignana Bharathi Institute of Technology, Hyderabad
Email: thoudishettivishwagna@gmail.com
[2]Assistant Professor, EEE Dept., Vignana Bharathi Institute of Technology, Hyderabad
Email: mamathakolluri@gmail.com

Abstract--This paper investigates the suitability of Inverse Sine Carrier Pulse Width Modulation (ISCPWM) for low-loss multimegawatt grid connected photovoltaic (PV) inverters. The proposed system is able to meet utilities regulations, IEEE and IEC standards. In an attempt to substantiate the potential superiority of ISCPWM over SHEPWM, this paper demonstrates that ISCPWM may allow grid-connected PV inverters to be controlled using a switching frequency of less than 1 kHz, while the inverter is still able to provide necessary operation features such as independent control of active and reactive powers and operation control simplicity. For system validation, Simulation results with ISCPWM are compared with the conventional SHEPWM technique. The advantages of the proposed technique include simplicity in implementation and flexibility in PWM waveforms. Simulation results demonstrate agreement, which validates the practicability of the proposed system.

Keywords: Grid-connected photovoltaic inverters, high power medium-voltage inverters, pulse width modulations (PWMs), switching losses.

1. INTRODUCTION

In the last two decades, environmental organizations have encouraged the power industry to use renewable power, such as wind, photovoltaic (PV), and tidal instead of fossil fuels as means to combat climate change. After years of research and development, wind and solar have proved to be more economical and technical feasible at a large scale, but they remain expensive compared to fossil fuels [1]–[4]. Rethinking of the whole power industry approach toward renewable power is on-going. Wind energy is widely accepted, with larger scale power plants compared to PV. The success of wind energy is driven by the willingness of governments with large wind potential to support the wind industry, and is not based on its superiority over PVs [2], [5].

This paper focuses on one aspect of solar energy, namely grid interfacing of large-scale PV farms. Power electronics interfacing of PV farms can be accomplished using pulse width modulated current source inverter (CSI) or voltage source inverter (VSI) [6]. Recently, the current source option for PV grid interfacing has been advocated as a mean of improving the effectiveness of maximum power tracking (MPT), as the number of series-connected PV in each string is reduced [7],

[8]. This reduces the impact of partial shading, and increases system efficiency by using one conversion stage instead of two stages, thereby benefiting from the voltage boost capability of the CSI (lower dc-link voltage and higher ac-side voltage) [9]–[14]. This approach may not be viable at high-power medium-voltage PV systems, since CSIs usually have higher semiconductor losses compared to VSIs of similar rating, switching frequency, and ac-side voltage. This is because the CSI has twice the semiconductors in the conduction path at any instant, compared to the VSI [15]–[17]. Additionally, CSI ability to meet strict grid codes, such as fault ride-through, is doubtful. The use of VSIs as interfacing units for grid integration of PV systems has been investigated intensively in the last five years. This includes the use of two-level and multilevel VSIs [18]–[20]. A multilevel VSI approach is not suitable for PV grid integration due to the following reasons: multilevel inverters with a common dc-link bus, such as diode and flying capacitor-clamped inverters, exacerbate the problem of partial shading as they require a large number of series-connected PV cells in order to build a relatively high dc voltage appropriate for medium-voltage applications [4], [21]–[26]. Although the modularity of the cascaded multilevel inverter is attractive for PV systems [27], [28], it exposes the PV cells to a low-frequency ac current component, hence reduces PV lifetime [6], [28]–[30]. Two-level VSI is widely used for grid-connected PV systems, regardless of the disadvantages such as high switching losses and relative low-quality output voltage waveforms [3]. Most grid-connected PV systems presented in the literature are inappropriate for high power due to the use of a high switching frequency (high switching losses and increased voltage stresses, *dv/dt,* on phase interfacing reactors and the transformer). Most of these studies adopt sinusoidal or space-vector pulse width modulation (PWM) to control the inverters. The use of sinusoidal PWM does not fully utilize dc-link voltage, thus lowering power density. Space vector modulation increases dc-link voltage and semiconductor utilization and improves power density compared to sinusoidal PWM, but may have difficulties operating in medium-voltage distribution systems where the possibility of unbalanced operation and ac faults is high. Digital implementation of these modulation strategies with grid-connected PV inverters necessitates the use of a relatively high switching frequencies for control purposes (the control period must be equal to the reciprocal of switching frequency).

Grid-connected PV inverters force the PV modules to operate at the maximum power point and present high-quality sinusoidal current and voltage to the grid [31], [32]. Normally, these inverters have to meet strict standards and grid codes [33]. For example, the current harmonic injection into the grid must not exceed 5%, with limitations imposed on individual harmonics as a percentage of the fundamental component—IEEE and IEC standards [34]. Typically, grid distortion is due to nonlinear loads and can be exacerbated by harmonics injected by poorly filtered grid-connected inverters. Therefore, the modulation strategy and coupling filtering are important aspects of inverter grid-connected renewable sources. Additionally, the IEEE and IEC standards also limit the maximum allowable dc current injection into the grid to avoid saturation of distribution transformers. This limit ranges from 12 % and 1% of the rated output current, as listed in Table I for low-voltage applications. The problem of dc current injection could be mitigated by improving circuit topologies or by including a line-frequency transformer between the inverter and the grid.

With regard to the mentioned priorities, in terms of modulation strategies and grid codes and standards requirements, medium-voltage applications sometimes favor the use of traditional modulation approaches such as selective harmonic elimination (SHE) and carrier-based PWM over space-vector modulation [35]–[38]. This paper investigates the possibility of using SHE to control high-power PV inverters in an attempt to suppress switching losses (by adopting switching frequencies of less than 1 kHz), improve dc-link voltage utilization, and reduced phase interfacing reactor *dv/dt* [36], [37], [39], [40]. To facilitate the inverter control process, the low-frequency output voltage switching waveforms produced using SHE are constructed using a relatively high sampling frequency, which is exclusively determined by the time required to execute the control algorithm in a DSP. The outcome of this investigation is substantiated using simulation and experimentation. For further demonstration of the potential advantages of SHE, this paper compares SHE simulation and experimental results to the results when the inverter is controlled using third-harmonic injection (THI) PWM that permits increased utilization of the dc-link voltage [41]. Moreover, this paper proposes a new method to improve SHE implementation, utilizing manipulation of the third-harmonic component in the phase voltage.

This paper is organized as follows: Section II discusses PWM techniques, namely SHE and third-harmonic PWM. This section also provides insight into manipulation of the third harmonic for spreading of the switching angles when the traditional SHE equations produce narrow angle ranges and its practical benefits. Section III discusses grid-connected inverter fundamentals from a power electronic system prospective and its control design when selective harmonic and THI PWM are used. Sections IV and V use simulation and experimentation results to demonstrate the viability of SHE PWM for high-power PV inverters. Section VI summarizes this paper and highlights its main contributions.

2. PWM FOR MULTIMEGAWATT GRID-CONNECTED INVERTERS
Normally, high-power medium-voltage grid-connected inverters for interfacing of renewable power plants tend to have priorities similar to those of HVDC converters. Some of these priorities are losses, and satisfaction of grid codes, IEEE and IEC standards. These priorities sometimes favor the use of traditional modulation approaches such as SHE [42], [43] and carrier-based PWM over the space-vector modulation for reasons outlined in Section I. Therefore, this paper investigates the possibility of using SHE to suppress conversion losses and reduce voltage stress on the phase interfacing reactor, by using a low switching frequency. This also improves the dc-link voltage and semiconductor switch utilization (maximum power extraction at reduced losses compared to space-vector or carrier based PWM from the same inverter and given dc-link voltage). Third-harmonic carrier-based PWM is considered in this paper to assist in the validation of the potential advantages of SHE.

A. SHE

Fig. 1(a) and (b) shows normalized output voltage (by 12*V*dc) of the two-level converter relative to the supply midpoint, when SHE is used to control the inverter, with three notches for fundamental voltage adjustment and elimination of the fifth and seventh harmonics. All switching angles for the arrangement in Fig. 1(a) (which will be referred to as solution 1) are located between 0 and 60∘ as shown in Fig. 1(c) (solid line). The maximum attainable modulation index for solution 1 is 1.1884. This maximum modulation index is achieved by solving an optimization problem that maximizes modulation index. The solution uses equations for the elimination of the fifth and seventh as nonlinear constraints, and *α1<α2, α2<α3* and *α3≤1/2π* as linear inequalities that maintain output voltage quarter-wave symmetry [44]–[46]. The arrangement in Fig. 1(b) (referred to as solution 2) produces switching angles distributed over 90∘, with *α2<α3* located between 60∘ and 90∘. The maximum modulation index with solution 2 is 1.16, which is lower than that produced by solution 1. Additionally, it can be observed that solution 2 produces a fundamental voltage 180∘ out of phase to that produced by solution 1, for the same fundamental voltage. This can be observed in Fig. 1(b) as during most of the first half cycle, the converter output phase is connected to the negative bus. This observation may be critical for SHE implementation in grid-connected applications. It is worth emphasizing that the arrangement for solution 2 always produces a smaller modulation index (hence fundamental voltage). Therefore, the choice between the arrangements may require careful attention to the fundamental voltage polarity. With the intention of extending the modulation index as the switching angle increases, this paper attempts to use adjustment of the third harmonic to decouple the maximum modulation index achievable from a given number of switching angles. When a fourth angle is added for third harmonic adjustment, the maximum modulation index using solution 1 remains at 1.1884 as shown in Fig. 1(f). This is obtained when the third-harmonic voltage magnitude ranges from 1/6 to 1/5 of the fundamental voltage. Notice that the control of the third-harmonic results in spreading of switching angles over the quarter of fundamental cycle (90∘)—see Fig. (d)–(f). Adjustment of the third harmonic in SHE does not result in decoupling of the modulation index from the number of switching angle; however, it remains useful at high modulation indices where standard SHE tends to produce switching angles in a narrow range close to zero (which cannot be realized practically). Injection of the third harmonic into arrangements 1 and 2 forces their switching angles to converge, for the same modulation index [see Fig. 1(g)]. For further confirmation of the potential usefulness of third-harmonic adjustment, the case with five notches where the fifth, seventh, and 11th harmonics are eliminated is presented in Fig. 1(h). With the adjustment of the third harmonic, arrangements 1 and 2 produce one unique solution that satisfies quarter-wave symmetry in the low modulation index range, *M<0.6*. Beyond this modulation index, the switching angles produced by solving the equations for arrangement 1 diverged from those produced by arrangement 2 [see Fig. 1(h)]. When the fifth, seventh, 11th, and 13th harmonics are eliminated, the switching angles associated with the seventh, 11th, and 13th remain the same for both solutions over the entire modulation index range, while those associated with first, third, and fifth diverge as modulation index increases [see Fig. 1(i)]. The addition of the third-harmonic equation to the set of nonlinear transcendental equations contributed to simplification of the solution process as it is easy to find one set of initial guesses that could be used to produce the solutions for the entire modulation index linear range. The Fourier coefficients for the generalized form of the waveforms in Fig. 1(a) and (b) are: $a_n = 0$, for all n; and $b_n = \frac{2V_{dc}}{n\pi}\left[2\sum_{k=1}^{N}(-1)^{k-1}\cos n\alpha_k - 1\right]$ in the case of the first arrangement that produces solution 1, and $b_n = \frac{2V_{dc}}{n\pi}\left[2\sum_{k=1}^{N}(-1)^{k}\cos n\alpha_k + 1\right]$ in case of the second arrangement that produces solution 2, for all odd values of n [47]–[49].
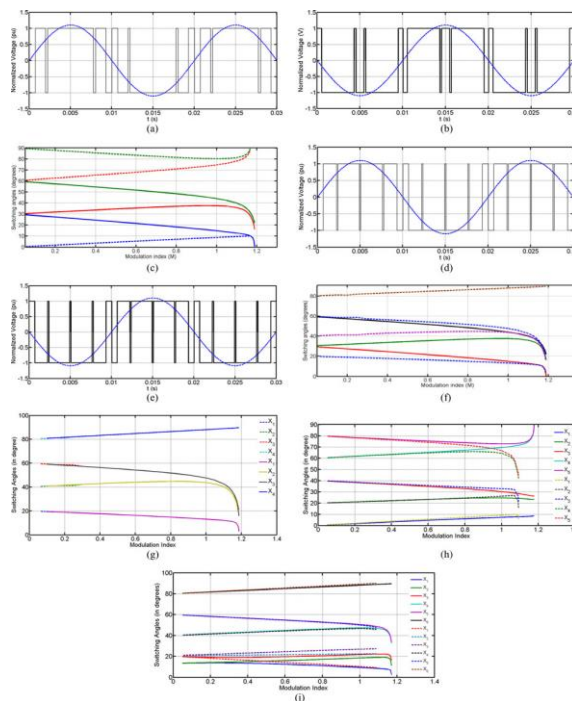

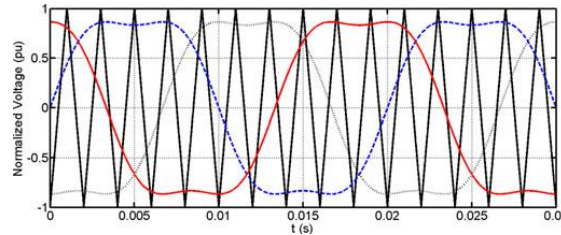**Fig. 1 Possible ways of implementing SHE.**

Fig. 2 Waveforms illustrating implementation of carrier-based THI PWM.

The modulation indices for the fundamental and third harmonic voltages are defined as $m = \frac{b_1}{\frac{1}{2}V_{dc}} = \frac{V_1}{\frac{1}{2}V_{dc}}$ and $m_3 = \frac{b_3}{\frac{1}{2}V_{dc}} = \frac{V_3}{\frac{1}{2}V_{dc}} = \frac{\gamma V_1}{\frac{1}{2}V_{dc}}$,where γ is a positive fraction used to describe the third-harmonic voltage component in terms of the fundamental. However, in this paper, all the experiments for the grid-connected inverter use nine switching angles in an attempt to meet harmonic requirements at the point of common coupling (PCC). Eight angles are used to eliminate non triplen harmonics up to the 25th harmonic. One of the attractive features that led to the adoption of SHE in this paper is that the magnitude of non triplen harmonics eliminated remains insignificant over the full modulation index linear range (0 to 1). Such a feature is not available in space-vector and carrier-based PWM.

B. THI PWM

Fig. 2 shows a natural sampling implementation of THI, with the magnitude of third harmonic equal to 1/6 the fundamental voltage. In this paper, third-harmonic-injected PWM is implemented based on regular sampling with a 2-kHz switching frequency (simulation and experimentation). This relatively high switching frequency is adopted to facilitate inverter control in the grid-connected mode.

C. PROPOSED ISCPWM

The control strategy uses the same reference (synchronized sinusoidal signal), as the conventional SPWM while the carrier triangle is a modified one. The control scheme uses an inverted sine (high frequency) carrier that helps to maximize the output voltage for a given modulation index. Enhanced fundamental component demands greater pulse area. The difference in pulse widths (hence area) resulting from triangle wave and inverted sine wave with the low (output) frequency reference sine wave in different sections can be easily understood. In the gating pulse generation of the proposed ISCPWM scheme shown in Fig.3, the triangular carrier waveform of SPWM is replaced by an inverted sine waveform.

For the ISCPWM pulse pattern, the switching angles may be computed as the same way as SPWM scheme. The equations of inverted sine wave are given by (6) and (7) for its odd and even cycles respectively. The intersections (ql, q2, q3... qi) between the inverted sine voltage waveform of amplitude 1 p.u and frequency f, and the sinusoidal reference waveform of amplitude Ma p.u and frequency fo can be obtained by substituting (1) in both (6) and (7). The switching angles for ISCPWM scheme can be obtained from (8) and (9).
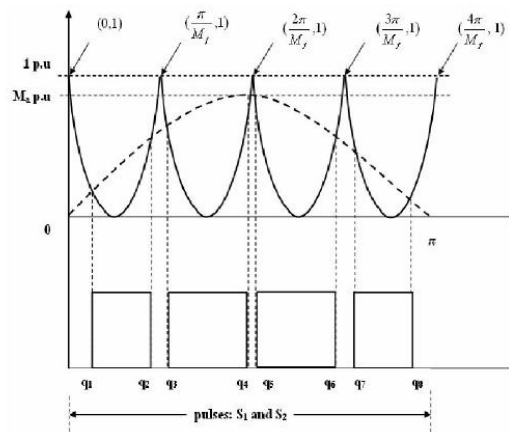

Fig 3 Inverted sine carrier PWM pulse pattern

$$y = 1 - \sin\left(M_f x - \frac{\pi}{2}(i-1)\right) \quad (1)$$

$$y = 1 - \sin\left(M_f x - \frac{\pi}{2}(i-2)\right) \quad (2)$$

$$M_a \sin q_t + \sin\left(M_f q_t - \frac{\pi}{2}(i-1)\right) = 1, \quad for\ i = 1,3,5... \quad (3)$$

　　　　　　　　　　　　97

$$M_a \sin q_i + \sin\left(M_f q_i - \frac{\pi}{2}(i-2)\right) = 1, \quad for \ i = 2,4,6\ldots$$

(4)

It is worthwhile to note that both in SPWM (considered) and ISCPWM schemes, the number of pulses will be equal to Mf and hence the constant switching loss is guaranteed. To have conceptual understanding of wider pulse area and hence the dexterous input dc utilization in the ISCPWM, location of switching angles, duty cycle and their dependence on Ma and Mf are discussed. Fig.4 depicts the influence of Ma on different switching angles (four angles considered in both cases) at a constant Mf of 6. From this figure, it is observed that the odd switching instants vary with negative slope and the even switching instants have positive slope. Variation of all the switching instants against Ma is the straight line and slope of each one is more than it's previous. All the odd switching angles of ISCPWM method happen earlier than similar angles of PWM method, while the situation is reverse in case of even switching angles and hence higher pulse area.
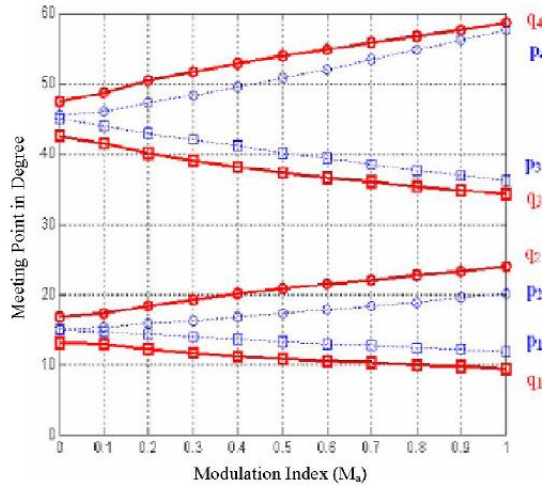
Fig.4 Influence Of Ma on Meeting Point

3. CONTROL SYSTEM AND FUNDAMENTAL OF GRID-CONNECTED INVERTERS

This section discusses the control systems of the grid connected inverter, and provides detailed discussion of the control variables that could be manipulated from a power electronic systems standpoint, including most of the possible physical limitations imposed by the ac-side passive elements which are not well documented. A generic phasor diagram and $P - Q$ envelope are presented that could be used to illustrate the operation of grid connected converters. Fig. 5 shows a schematic diagram of a three-phase VSI connected to grid through an LC filter and interfacing transformer. The active and reactive powers are regulated using direct power control, where the filter bus voltage is assumed constant. Inverter power injection into the grid is regulated in the synchronous reference frame, where the voltage magnitude at the filter bus is aligned with the d-axis (the reference for the whole system, in other words all measurements in the dq axes will be relative to the filter bus voltage). Based on this principle, the inverter ac-side dynamic can be expressed in the dq axes as follows:

$$\frac{dI_{fd}}{dt} = -\frac{R_f}{L_f} I_{fd} + \frac{[V_{cd} - V_{fd} + \omega L_f I_{fq}]}{L_f}$$

(5)

$$\frac{dI_{fq}}{dt} = -\frac{R_f}{L_f} I_{fq} + \frac{[V_{cq} - V_{fq} - \omega L_f I_{fd}]}{L_f}$$
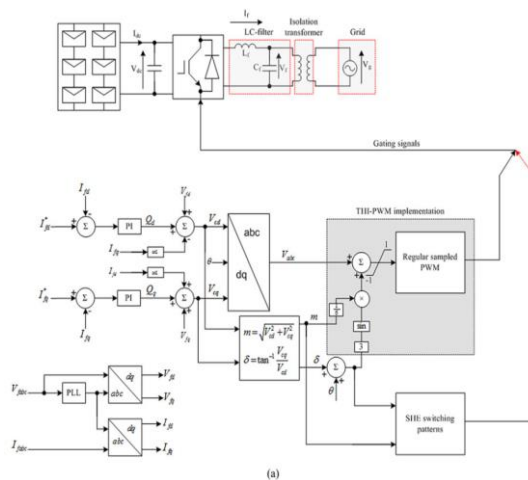
(6)

(a)

Fig. 5 Schematic diagram of a grid-connected PV inverter with SHE and THI PWM

4. SIMULATION RESULTS

The simulation circuit of multi megawatt photovoltaic inverters configuration Figure. 6. The simulation circuit of conventional SHEPWM based control strategy is shown in Fig.7. The simulation circuit of proposed ISCPWM based control strategy is shown in Fig.9.
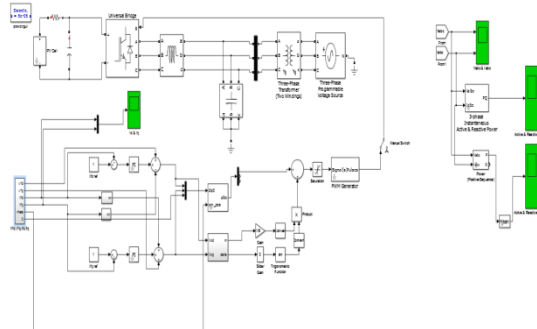

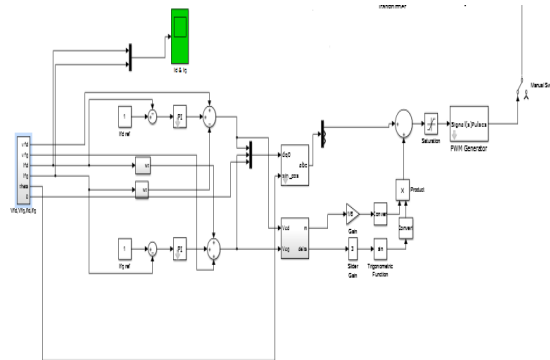**Fig. 6 Simulation Circuit of Conventional System**

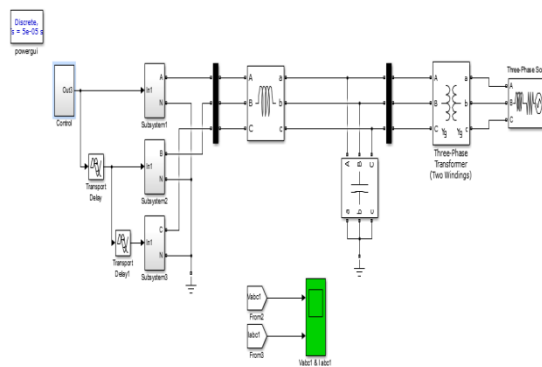**Fig. 7 Simulation of SHEPWM Based Control Strategy**
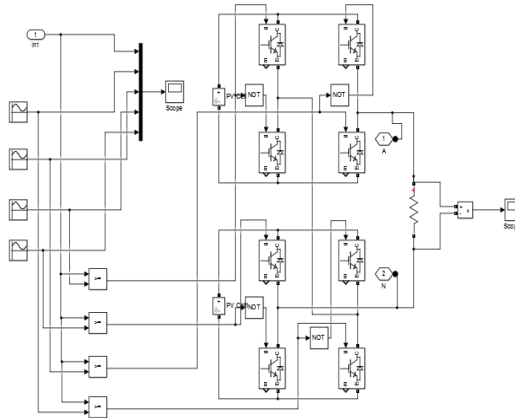

Fig. 8 Simulation Circuit of Proposed System

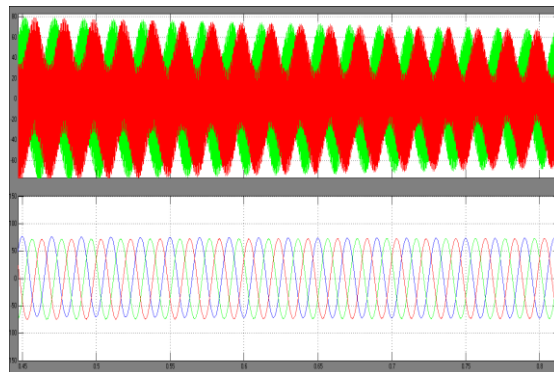**Fig. 9 Simulation of ISCPWM Based Control Strategy**

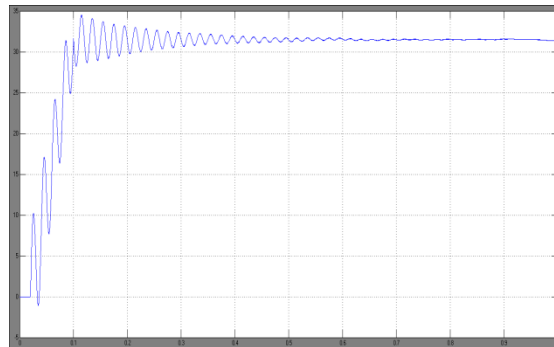**Fig.10 Grid Voltages and Currents with Conventional System**
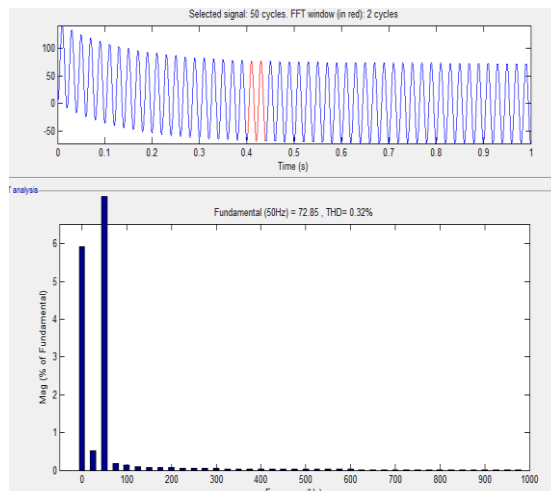

Fig.11 Active Power of Grid with Conventional System

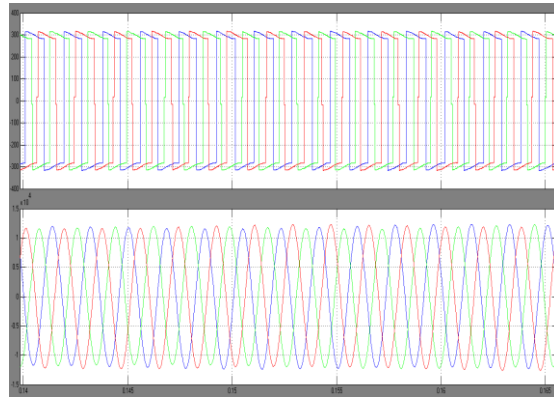**Fig.12 THD Spectrum of Grid Currents**

Fig.13 Voltages and Currents with Proposed System

5. CONCLUSION

This paper investigated the suitability of SHEPWM and ISCPWM, which is established in machine drives applications, applied to high-power medium-voltage grid-connected inverters used as interfacing units for large-scale integration of renewable energy sources. It has been demonstrated that ISCPWM does not compromise any grid-connected inverter functionalities normally provided when controlled using carrier-based PWM strategies. Additionally, this paper has established that contrary to traditional SHE implementation, with adjustment of the third harmonic magnitude, a universal

solution for harmonic elimination equations evolves that generally spreads the switching angles over $90°$. A comparison between both the modulation techniques has been done.

REFERENCES

[1] J. P. Benner and L. Kazmerski, "Photovoltaics gaining greater visibility," IEEE Spectr., vol. 36, no. 9, pp. 34–42, Sep. 1999.
[2] C. Zhe, J. M. Guerrero, and F. Blaabjerg, "A review of the state of the art of power electronics for wind turbines," IEEE Trans. Power Electron., vol. 24, no. 8, pp. 1859–1875, Aug. 2009.
[3] Y. Bo, L.Wuhua, Z. Yi, and H. Xiangning, "Design and analysis of a grid connected photovoltaic power system," IEEE Trans. Power Electron., vol. 25, no. 4, pp. 992–1000, Apr. 2010.
[4] J. Ebrahimi, E. Babaei, and G. B. Gharehpetian, "A new topology of cascaded multilevel converters with reduced number of components for high-voltage applications," IEEE Trans. Power Electron., vol. 26, no. 11, pp. 3109–3118, Nov. 2011.
[5] X.Hailiang, H. Jiabing, and H.Yikang, "Operation of wind-turbine-driven DFIG systems under distorted grid voltage conditions: Analysis and experimental validations," IEEE Trans. Power Electron., vol. 27, no. 5,
pp. 2354–2366, May 2012.
[6] J.A.Houldsworth and D.A.Grant, "The Use Harmonic Distortion to Increase the Output Voltage of Three-Phase PWM Inverter," IEEE Transaction on Industry Application, vol.1 IA-20, pp. 1224- 1228, Sept/Oct 1984.
[7] K.Taniguchi, Y.ogino and H.Irie, "PWM Technique for Power MOSFET Inverter," IEEE Transactions on Power Electronics, vol.3, no.2, p.p328-334, July 1988.
[8] Kjeld Thorborg and Ake Nystrom, "Staircase PWM: An Uncomplicated and Efficient Modulation Techniques for AC Motors Drives", IEEE Transactions on Power Electronics, vol.3, no.4, pp.391-398, Oct. 1988.
[9] S.Jeevananthan, P.Dananjayan and S.Venkatesan,"SPWM-An Analytical Characterization, and Performance Appraisal of Power Electronic Simulation Software's", Proceedings of PEDS2005, Kulala Lumpur, Malasia, pp.681-686, Nov.28-Dec. 1, 2005.
[10] W.G.Dunford and J.D.Van Wyk, "The Calculation of Sub-Harmonics in an Asynchronous PWM Induction Motor Drive," Proceedings of IEEE PESC Conference Record, pp.672-677, 1990.

Thoudeshetti Vishwagna received B.Tech Degree in Electrical and Electronics Engineering from Jyothismathi Institute of Technology And Science (JNTUH) in the year of 2012. She is currently M.Tech student in the stream Power Electronic and Drives. Vignana Bharathi Institute of Technology, Hyderabad, India. And she is interested in the field of Power Electronics.
Email: thoudishettivishwagna@gmail.com

K. Mamatha is currently working as a Assistant Professor in Vignana Bharathi Institute of Technology, Hyderabad, India. Her research areas include Control Systems, Power Electronics &Drives, Power Systems and Basic Electrical Engineering.
Email: mamathakolluri@gmail.com